

Incommensurate Spin Density Wave versus local magnetic inhomogeneities in $\text{Ba}(\text{Fe}_{1-x}\text{Ni}_x)_2\text{As}_2$: a ^{57}Fe Mössbauer spectral study

A Olariu, P Bonville, F Rullier-Albenque, D Colson and A Forget

Service de Physique de l'Etat Condensé, Orme des Merisiers, IRAMIS, CEA-Saclay (CNRS URA 2464), 91191 Gif sur Yvette Cedex, France

E-mail: pierre.bonville@cea.fr

Abstract. We report ^{57}Fe Mössbauer spectral results in pure and doped $\text{Ba}(\text{Fe}_{1-x}\text{Ni}_x)_2\text{As}_2$ with $x = 0.01$ and 0.03 . We show that all these materials present a first-order magnetic transition towards a magnetically ordered state. In the doped compounds, a broad distribution of Fe hyperfine fields is present in the magnetic phase. We successfully fit the Mössbauer data in $\text{Ba}(\text{Fe}_{1-x}\text{Ni}_x)_2\text{As}_2$ in the framework of two different models: 1) an incommensurate spin density wave; 2) a dopant-induced perturbation of the Fe polarization, recently proposed to interpret ^{75}As NMR data in $\text{Ba}(\text{Fe}_{1-x}\text{Ni}_x)_2\text{As}_2$, which is valid only in the very dilute limit $x = 0.01$. Moreover, we show here that these NMR data can also be successfully analysed in terms of the “incommensurate model” for all doping contents by using the parameters obtained from the Mössbauer spectral analysis. Therefore it is not possible to rule out the presence of an incommensurate spin density wave on the basis of the ^{75}As NMR data.

PACS numbers: 74.70.Xa, 75.30.Fv, 76.80.+y, 76.60.-k

Submitted to: *New J. Phys.*

1. Introduction

The nature of magnetism in the recently discovered iron pnictides superconductors [1] is an intensively studied topic, due to its possible coexistence with superconductivity and relation to the pairing mechanism [2]. In the so-called “122 family”, the parent compounds AFe₂As₂, where A=Ba, Ca, Sr or Eu, present a transition to a spin density wave (SDW) phase which is commensurate with the lattice spacing. When substituting Fe with another metal, like Co or Ni (the dopant), the Néel temperature gradually decreases and superconductivity eventually emerges at higher dopant concentrations. In Ba(Fe_{1-x}Co_x)₂As₂, superconductivity and magnetism coexist locally below the critical temperature T_c [3, 4], i.e. there occurs a so-called mixed phase with spatial coexistence of the two phases. By contrast, in some pnictides belonging to another family, e.g. LaFeAsO_{1-x}F_x [5], magnetism vanishes when superconductivity sets in. Magnetic order in all AFe₂As₂ is antiferromagnetic (AF) and the spin arrangement is formed by AF stripes along \mathbf{a} and ferromagnetic stripes along \mathbf{b} , in the orthorhombic notation [6]. The Fe ordered moment is small, of the order of $1 \mu_B$, which, together with the metallic behavior in the normal state, suggests the presence of itinerant magnetism. This is believed to be induced by a Fermi surface instability driven by the nesting between an electron and a hole pocket [7, 8], as seen by angle-resolved photoemission studies (ARPES) in BaFe₂As₂ [9], as well as in electron-doped Ba(Fe_{1-x}Co_x)₂As₂ [10] and hole-doped Ba_{1-x}K_xFe₂As₂ [11, 12].

In doped systems, it was suggested that an imperfect nesting between the hole and electron pockets should lead to the formation of an incommensurate spin density wave (IC-SDW) below the magnetic transition temperature [13], as occurs in Cr [14]. Several theoretical studies have shown that coexistence of superconductivity and magnetism is favoured by the presence of an IC-SDW [15, 16, 17]. Therefore, the observation of an IC-SDW is an important issue to verify the various theories put forward in order to describe the physics of pnictide superconductors. Experimentally, a phase transition from commensurate to incommensurate SDW was recently reported in SrFe₂As₂ under pressure [18], based on NMR measurements. In Ba(Fe_{1-x}Co_x)₂As₂, the presence of an IC-SDW was inferred from local techniques such as NMR [3], Mössbauer spectroscopy [19] and μ SR [20], but was not observed by neutron scattering [21, 22] until recently, and only in a narrow concentration range close to a Co doping level $x=0.055$ [23]. Therefore, it was claimed that the perturbation of magnetic order induced by the dopant is responsible for the effects observed in Refs.[3, 19]. In Ba(Fe_{1-x}Ni_x)₂As₂, ⁷⁵As NMR lineshapes were interpreted in the framework of an empirical model according to which the magnetic order is commensurate, and the dopant induces perturbations of the Fe moment amplitude [24, 25]. In Ba(Fe_{1-x}Rh_x)₂As₂, Mössbauer spectra were interpreted assuming either an IC-SDW or the presence of disorder [26], while neutron scattering did not detect any incommensurability in this family [27].

In this paper, we present Mössbauer results obtained on a powder sample of BaFe₂As₂ and in single crystal mosaics of Ba(Fe_{1-x}Ni_x)₂As₂ with $x=0.01$ and 0.03 .

In the doped systems, we show that a distribution of Fe hyperfine fields is present in the magnetic phase, similar to what was observed in Ba(Fe_{1-x}Co_x)₂As₂ [19]. We interpret the Mössbauer data using the two models for an incommensurate spin density wave and for a dopant-induced Fe moment perturbation. Then, we present simulations of NMR spectra from Refs.[24, 25] assuming an IC-SDW modulation with the parameters obtained from the fit of the Mössbauer spectra. This is motivated by the observation made in Ref.[24] that the NMR data rule out the presence of IC-SDW in Ni doped compounds.

2. Experimental and sample characterization

BaFe₂As₂ in powder form was prepared by solid-state reaction and it presents a magnetic transition at $T_{\text{SDW}} \sim 139.5$ K [28]. Single crystals of Ba(Fe_{1-x}Ni_x)₂As₂ with $x = 0.01$ and 0.03 were grown by the self-flux method, as described in detail in Ref.[29]. The system is not superconducting at $x = 0.01$, while at $x = 0.03$ superconductivity occurs below $T_c \simeq 11$ K. Susceptibility measurements on a single crystal show that the whole sample is superconducting below T_c . Resistivity measurements performed on crystals from the same batches showed them to be very homogenous [29], with a magnetic transition towards a spin density wave at $T_{\text{SDW}} \simeq 112.5$ K for $x = 0.01$ and $\simeq 47$ K for $x = 0.03$. Ni-doped platelet-like crystals were glued in mosaic on aluminium scotch tape with the (a, b) plane perpendicular to the γ beam. The scotch tape contains iron impurities in very small amounts, which give rise to a quadrupolar doublet with 0.07% resonant absorption. Because the resonant absorption due to the BaFe₂As₂ phase is around 2%, the iron impurities give a negligible contribution to the spectra. Spectra were recorded using a commercial ⁵⁷Co*:Rh γ -ray source mounted on an electromagnetic drive with linear velocity signal. The width calibration of the source was done with a thin K₄Fe(CN)₆ · 3H₂O absorber and the half width at half maximum (HWHM) is found to be 0.128 mm/s. The velocity and linearity calibration were performed with an enriched α -Fe₂O₃ absorber and a commercial Wissel laser interferometer. All spectra are shown in a velocity range of ± 2 mm/s. However, the spectra in pure BaFe₂As₂ and the 4.2 K spectrum in Ba(Fe_{0.99}Ni_{0.01})₂As₂ were recorded in a velocity range of ± 3 mm/s.

3. BaFe₂As₂

In the high temperature paramagnetic range, the Mössbauer spectra are well fitted by a single Lorentzian-shaped line of HWHM 0.15 mm/s. In the magnetically ordered phase below $T_{\text{SDW}} \simeq 139.5$ K (Fig.1) and up to about 125 K, spectra are well fitted to a 6-line pattern due to a single hyperfine field of 5.4 T at 4.2 K. This is expected for a commensurate magnetic order and it is in good agreement with similar measurements presented in Refs.[30, 31, 32], as well as with neutron scattering [33] and NMR [34] results. A peculiarity of these hyperfine field spectra is that the HWHM of the middle lines, 0.134(4) mm/s, is equal within uncertainties to that of the inner lines, while the

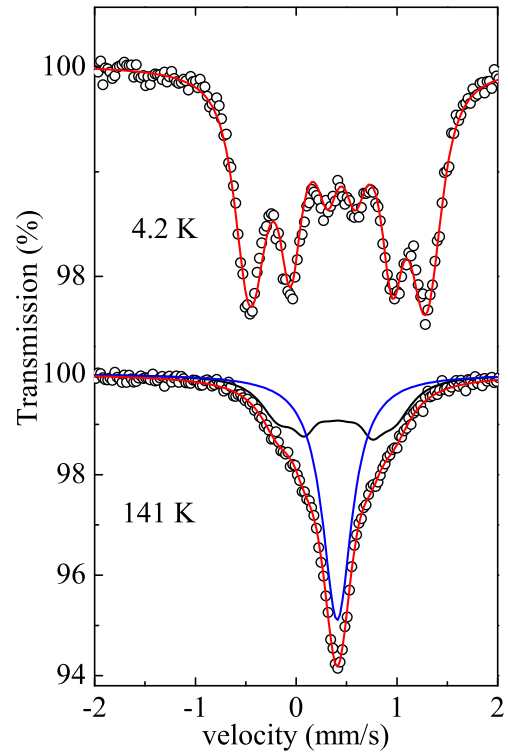


Figure 1. Mössbauer absorption spectra on ^{57}Fe in $BaFe_2As_2$ in the SDW phase (4.2K) and close to the SDW to paramagnetic transition (141K). Lines are fits as described in the text.

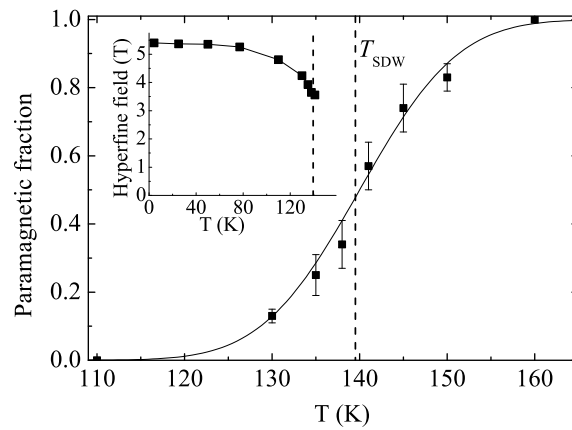


Figure 2. Temperature dependence of the paramagnetic fraction in $BaFe_2As_2$ around T_{SDW} , extracted from the fit of the Mössbauer spectra. The vertical dashed lines indicate $T_{SDW} \simeq 139.5$ K. Inset: temperature dependence of the hyperfine field. The lines are guides for the eye.

HWHM of the outer lines is 0.168(4) mm/s, significantly larger. This unusual spectral effect is observed in other published spectra at 4.2 K [30, 31] and it cannot be due to a mere distribution of hyperfine fields, which would yield increasing broadenings for the inner, middle and outer lines. It can be accounted for by correlated distributions of quadrupolar interaction (QI) and isomer shift (IS). The presence of a QI distribution at the ⁵⁷Fe site is in line with the ⁷⁵As NMR spectra in BaFe₂As₂, which indicate a sizeable distribution of quadrupolar frequencies at the As site [34]. Correlated distributions of QI and IS have been observed in amorphous or glassy materials [35, 36], but they are not expected in an ordered metallic material such as BaFe₂As₂. We note that they can be inferred to occur in charge density wave (CDW) phases, but such a phase has not been reported in the iron pnictides.

The thermal variation of the hyperfine field is shown in the inset of Fig.2. Its weak temperature dependence suggests a transition with first order character. In the temperature range from 130 to 150 K close to T_{SDW} , the spectra cannot be fitted to a single sextet. An additional single-line paramagnetic component develops at the expense of the magnetically ordered one as temperature increases above 120 K. The fit with two components obtained at 141 K is shown in Fig.1. The presence of this relatively narrow magnetic/paramagnetic coexistence region (see Fig.2) is another indication of the first order character of the transition. This is in good agreement with the ⁷⁵As NMR data in BaFe₂As₂ [34]. In BaFe₂As₂, the paramagnetic fraction develops from 0 to 100% over a 15 K range on each side of the transition ($\pm 0.1T_{\text{SDW}}$). This is quite different from the behaviour in Co-doped systems, where coexistence is observed to occur on a much wider temperature range [19], up to about 1.5 T_{SDW} above the magnetic transition.

4. Ba(Fe_{1-x}Ni_x)₂As₂

4.1. Interpretation of Mössbauer spectra

Mosaic Mössbauer spectra obtained for Ba(Fe_{1-x}Ni_x)₂As₂ with $x=0.01$ and 0.03 with the γ -beam along the c axis are shown in Fig.3 for $T = 4.2$ K. These spectra do not display the six narrow line pattern expected for a single magnetic environment, as in the undoped compound. This indicates a distribution of Fe hyperfine fields, similar to what was observed in Ba(Fe_{1-x}Co_x)₂As₂ [19]. Our data is in agreement with that reported in Refs.[32, 37] for the Ni content $x=0.016$ and 0.024. In these works, the spectra were fitted to a superposition of commensurate and sine-wave incommensurate subspectra [38]. Here, we fit the spectra assuming either an incommensurate spin density wave with several harmonics, or a dopant-induced perturbation model. We focus mostly on the $x = 0.01$ Ni concentration in order to take advantage of the good resolution of the spectra. For $x \geq 0.016$, due to the decrease of the Fe magnetic moment, spectra become almost featureless and therefore lack the resolution necessary for our analysis.

Spectra can be very well fitted by assuming an incommensurate modulation of the Fe moments with several harmonics (Fig.3, left panel) as described in Ref.[19].

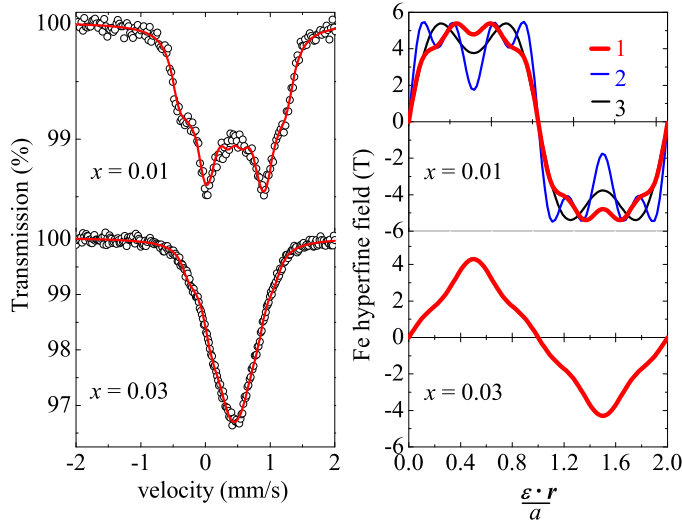


Figure 3. **Left:** Mössbauer spectra in $Ba(Fe_{1-x}Ni_x)_2As_2$ obtained at 4.2 K for $x=0.01$ and 0.03. Continuous lines are fits assuming an incommensurate modulation of Fe moments. **Right:** modulations that fit well the spectra shown in the left panel, with parameters from Table I. The thick red lines correspond to the fits shown on the left.

According to this model, the hyperfine field H_{hf} can be developed as a Fourier series along the propagation vector $\boldsymbol{\epsilon}$ of the incommensurate modulation:

$$H_{hf}(\boldsymbol{\epsilon} \cdot \mathbf{r}) = \sum_{k=0}^n h_{2k+1} \sin[(2k+1) \frac{\pi}{a} \boldsymbol{\epsilon} \cdot \mathbf{r}]. \quad (1)$$

The fit of the Mössbauer spectra allows us to extract the parameters h_{2k+1} . Due to the local character of the technique, the vector $\boldsymbol{\epsilon}$ cannot be determined. Fourier coefficients obtained for $x=0.01$ and 0.03 are given in Table I and the corresponding modulations are shown in Fig. 3 (right panel). Note that there are several sets of parameters that yield equally good fits of the spectra. The shape of the modulation appears to evolve with doping: for $x = 0.01$ it is close to a "square-wave" while it approaches a sine-wave for $x = 0.03$, similar to $Ba(Fe_{1-x}Co_x)_2As_2$. The relative intensities of the lines are close to 3:4:1:1:4:3, as expected when the hyperfine field, and thus the Fe magnetic moment, is perpendicular to the γ -beam. This is in good agreement with neutron scattering measurements in $Ba(Fe_{1-x}Ni_x)_2As_2$ at low doping levels, showing that moments are parallel to \mathbf{a} as in pure $BaFe_2As_2$.

So far we have shown that the hypothesis of IC-SDW leads to very good fits of the Mössbauer spectra. We now show that good fits can also be obtained with the empirical model described in Ref.[24], based on first-principle calculations [39], assuming that the dopant induces a perturbation of the Fe moment amplitude. Within this model, the Fe moment value $m(\mathbf{r})$ at distance \mathbf{r} from the origin, is given by the expression:

$$m(\mathbf{r}) = m_0 \Phi_x(\mathbf{r}) \cos(\mathbf{Q}_0 \cdot \mathbf{r}), \quad (2)$$

Table 1. Fourier coefficients (in T) obtained for Ni-doping with $x = 0.01$ (three sets yielding equally good fits) and $x = 0.03$ (only one set is shown, although several sets fit the data equally well).

x	N ^o	h_1	h_3	h_5	h_7
0.01	1	5.95	1.04	0.312	0.444
0.01	2	5.30	2.60	0.486	1.45
0.01	3	5.69	1.93	0	0
0.03	-	3.61	-0.43	0.26	0

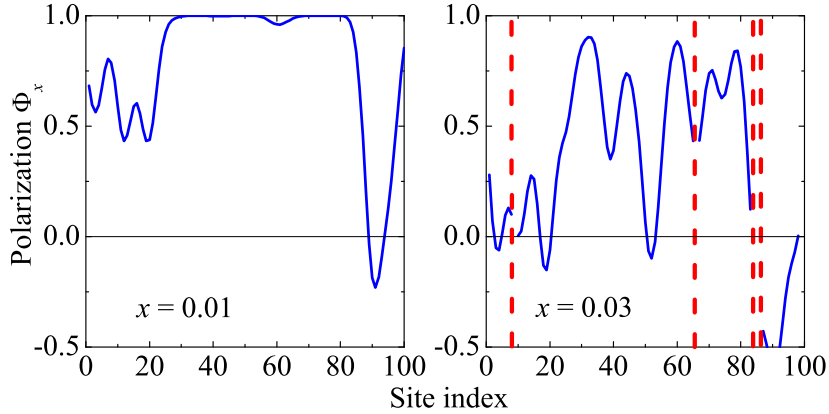


Figure 4. Fe spin polarization calculated, for $x=0.01$ and 0.03 , in the framework of the “perturbation” model along a line in the (\mathbf{a}, \mathbf{b}) plane parallel to \mathbf{a} . We use expression (2) with parameters $\alpha=0.6$ and $\lambda = 2.5a$. The red dashed lines mark the positions of the dopant atoms. According to this model, the periodicity of the magnetic structure should be completely broken for $x=0.03$, in disagreement with neutron scattering results.

where $\Phi_x = 1 - \alpha \sum_i \exp[-(\mathbf{r} - \mathbf{r}_i)^2/\lambda^2]$. In this latter expression, \mathbf{r}_i is the distance to the i th dopant atom, the sum runs over all dopant atoms and $\mathbf{Q}_0 = \frac{\pi}{a}(1, 0, 1)$ is the SDW vector for the commensurate pattern observed in $BaFe_2As_2$. The parameter α gives the reduction of the spin of the dopant atoms, while λ describes the spatial extent of the perturbation and m_0 is an unperturbed Fe moment. This model allows one to reproduce correctly the ^{75}As NMR spectra for different Ni concentrations [24], with parameters $\alpha = 0.6$ and $\lambda = 2.5a$. In the following, we shall refer to this model as the “perturbation” model.

In order to visualize the effect of the dopant atom on its magnetic environment within this model, we chose a (300×300) point mesh representing one Fe-As (\mathbf{a}, \mathbf{b}) plane and placed Ni atoms at random in this plane according to the concentration.

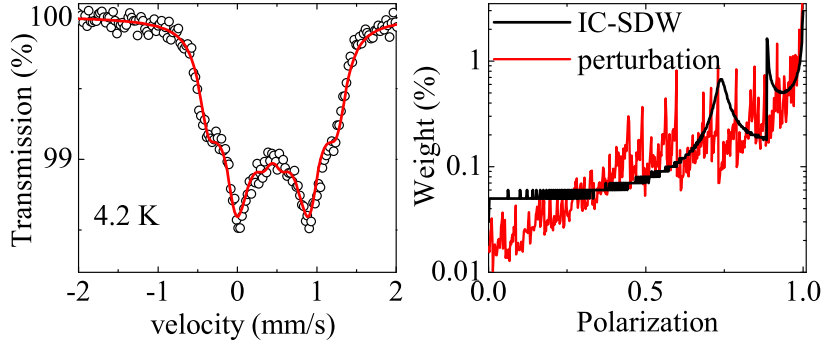


Figure 5. **Left:** Mössbauer spectrum at 4.2 K for $Ba(Fe_{1-x}Ni_x)_2As_2$ with $x = 0.01$, fitted to the “perturbation” model. **Right:** histogram of the reduced Fe polarizations for the IC-SDW and “perturbation” models for $x=0.01$.

We compute the Fe polarization along a given direction as a function of the distance from the origin for $x=0.01$ and 0.03 (Fig.4). For $x = 0.01$, the polarization remains close to 1 for most sites, although destructive interferences lead to a few Fe sites with strongly depleted or zero moments. For $x = 0.03$, this model leads to an average polarization much smaller than 1 and even negative for a few sites. The disorder induced by the presence of Ni dopants would be so strong that the periodicity of the magnetic structure would be completely broken. If this were the case, no magnetic order could have been detected by neutron scattering. However, Bragg peaks are clearly observed at concentrations close to $x = 0.03$ [40], which shows that the model is not valid beyond the very dilute limit. Note that for even larger dopant content, the polarization of all sites would turn negative and smaller than -1, which is unphysical. We therefore restricted our simulations of the Mössbauer spectra to $x = 0.01$. Good agreement with the data was found for this concentration for a wide range of parameter values, with α varying from 0.4 to 0.8 and λ from $2a$ to $3a$. The obtained fit is shown in the left panel of Fig.5 for $\alpha = 0.6$ and $\lambda = 2.5a$. Note that even for $x = 0.01$, the rather large values of α and λ seem to overestimate the influence of magnetic disorder with respect to what is predicted by theoretical calculations [39].

One can wonder why both the IC-SDW and “perturbation” models reproduce the Mössbauer spectra well. This is in fact due to similar features of the distributions of Fe hyperfine fields for both models, as shown in the right panel of Fig.5. Both histograms are very asymmetric, with a quasi-divergence at the maximum field value and a continuous distribution extending down to zero polarisation. For the “perturbation” model, the noise is due to the random lattice positions of the dopant atoms.

Spectra recorded at higher temperatures for $x = 0.01$ are shown in Fig.6. All the spectra measured below $T_{SDW} \simeq 112.5$ K can be well fitted either with the IC-SDW or the “perturbation” model with the parameters $\alpha = 0.6$ and $\lambda = 2.5a$, as described above. The IC-SDW model yields systematically better fits with $\chi^2 \sim 1.10 - 1.25$, while fits with the “perturbation” model have $\chi^2 \sim 1.5 - 2$. However, this is not very significant because

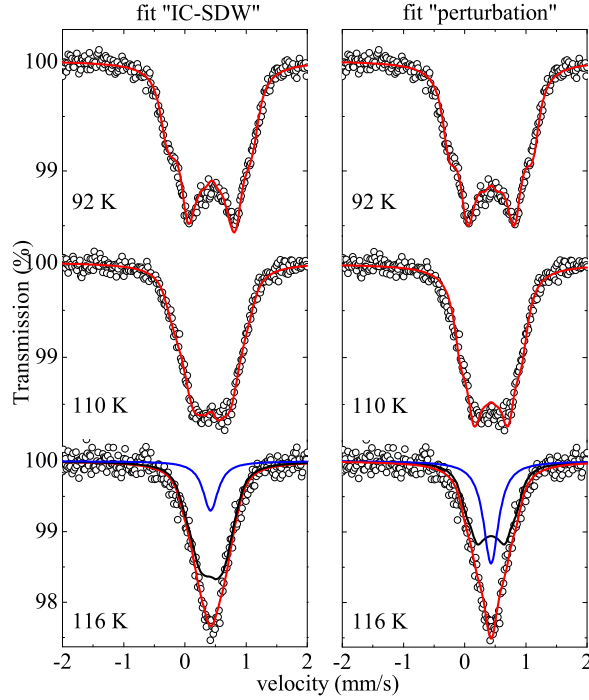


Figure 6. Mössbauer spectra at different temperatures for $\text{Ba}(\text{Fe}_{1-x}\text{Ni}_x)_2\text{As}_2$ with $x = 0.01$. Continuous lines are fits assuming either an incommensurate modulation (left panel) or an dopant-induced distribution of the Fe hyperfine field (right panel). At 116 K, a Lorentzian-shaped component was added to the fit in order to represent the paramagnetic fraction of the sample.

the IC-SDW model involves more parameters. Fits with the IC-SDW model yield similar shapes of the modulations in the temperature range from 4.2 to 110 K. Above T_{SDW} determined by resistivity measurements, a paramagnetic component develops at the expense of the magnetic one in a temperature range of $0.1T_{\text{SDW}}$, similar to pure BaFe_2As_2 , indicative of a first order transition. The paramagnetic fraction, shown as a function of temperature in Fig.7, grows rapidly with T , so that at $T \sim 120$ K the sample is almost fully paramagnetic. Note that when the fraction of the magnetic phase is less than $\sim 50\%$, it is impossible to perform an accurate quantitative determination of the paramagnetic fraction, due to the lack of spectral resolution. Therefore, no experimental data are shown for temperatures above 118 K. In the temperature range from 110 to 116 K, fits with the IC-SDW model were performed by assuming that the shape of the modulation does not evolve with T , in order to limit the number of fitting parameters. Hysteresis is observed between warming and cooling procedures. This, together with the step decrease of the hyperfine field when approaching T_{SDW} (Fig.7 inset), confirms the first order nature of the transition. Here the hyperfine field H_{hyp} was derived from the fit with both the “perturbation” and IC-SDW models. In the former case, H_{hyp} is a free parameter proportional to m_0 . In the latter case, H_{hyp} is the average over a period

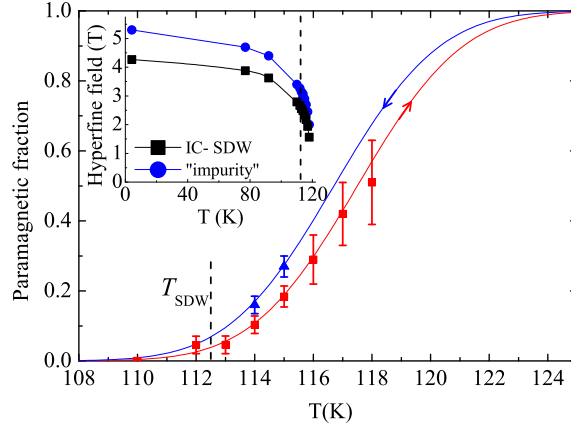


Figure 7. $Ba(Fe_{1-x}Ni_x)_2As_2$ with $x = 0.01$: temperature dependence of the paramagnetic fraction for increasing and decreasing temperature, derived from the fit of Mössbauer spectra with an IC-SDW. Inset: temperature dependence of the hyperfine field, obtained from both fits with an IC-SDW and dopant-induced perturbation. The vertical dashed lines indicate $T_{SDW} \simeq 112.5$ K. Lines are guides for the eye.

of the incommensurate modulation, given by the expression:

$$H_{hyp} = \left(\frac{1}{2} \sum_k h_{2k+1}^2 \right)^{0.5} \quad (3)$$

We also fitted the spectrum recorded at 4.2 K in $Ba(Fe_{1-x}Co_x)_2As_2$ [19] for $x=0.014$ to the “perturbation” model. A rather good fit is obtained (not shown) with parameters $\alpha \simeq 0.37$ and $\lambda \simeq 2.5a$. The value of λ which describes the extent of the spatial distribution is found to be the same as for Ni doping.

4.2. Simulations of ^{75}As NMR spectra assuming an IC-SDW

We have shown in the previous section that, in $BaFe_2As_2$ doped with Co or Ni, the ^{57}Fe Mössbauer spectra can be equally well reproduced assuming either an IC-SDW or a dopant-induced perturbation model. So the Mössbauer spectra do not allow us to distinguish between the two. Recently, it was claimed that the IC-SDW assumption yielded poor fits to the ^{75}As NMR spectra in Ni doped $BaFe_2As_2$ [24, 25], and that this fact favoured the “perturbation” model. In these latter works, the simulations of the NMR spectra with the IC-SDW assumption were carried out using the incommensurate modulation inferred from the NMR data at $x=0.06$ Co-doping [3]. Here, we perform simulations of the NMR spectra with the incommensurate modulations derived from the Mössbauer spectra and we show that good agreement is achieved.

We consider a plane with (500×500) Fe sites and calculate, for each As site, the corresponding hyperfine field. The ^{75}As hyperfine Hamiltonian can be written as:

$$\mathcal{H}_{hf} = \gamma \hbar \hat{\mathbf{I}} \cdot \sum_i \mathbb{B}_i \cdot \mathbf{m}(\mathbf{r}_i). \quad (4)$$

Here the sum runs over the four Fe nearest neighbors of an As nucleus with moment \mathbf{m} , γ is the gyromagnetic ratio of ^{75}As ($\gamma = 7.292 \text{ MHz/T}$), $\hat{\mathbf{I}}$ is the nuclear spin operator and \mathbb{B} the hyperfine tensor. Four hyperfine tensor components are known: $B_{aa} = B_{bb} = 0.88 \text{ T}/\mu_B$, $B_{cc} = 0.47 \text{ T}/\mu_B$ and $B_{ac} = 0.43 \text{ T}/\mu_B$, determined previously in pure $BaFe_2As_2$ [34]. The fifth component B_{ab} is unknown, but it has to be taken into account when the external field is perpendicular to the \mathbf{c} axis ‡. The Fe magnetic moment at position \mathbf{r} is given by:

$$m(\mathbf{r}) = m_0 \cos(\mathbf{Q}_0 \cdot \mathbf{r}) \sum_{k=0}^n \frac{h_{2k+1}}{h_1} \sin[(2k+1)\frac{\pi}{a}\boldsymbol{\epsilon} \cdot \mathbf{r}], \quad (5)$$

the total propagation vector being $\boldsymbol{\tau} = \mathbf{Q}_0 + \frac{\pi}{a}\boldsymbol{\epsilon}$. The parameters h_{2k+1} are known from the Mössbauer spectra, therefore the free parameters are $\boldsymbol{\epsilon}$, m_0 and B_{ab} .

In Fig.8 we show the NMR spectra from Refs.[24, 25] for two samples in the low doping regime, with the external field parallel to the \mathbf{c} axis or along [110]. Simulations with the dopant-induced perturbation model are shown as dashed lines, with parameters $\alpha = 0.6$ and $\lambda = 2.5a$. The quadrupolar frequency was taken as $\nu_Q = 2.0 \text{ MHz}$ and the magnetic moments were $0.77 \mu_B$ for $x = 0.0072$ and $0.65 \mu_B$ for $x = 0.026$.

For the simulations of the NMR spectra for $x = 0.0072$ assuming IC-SDW, we considered the modulation corresponding to the $x=0.01$ Mössbauer spectrum. The best fits to the NMR spectra were found with the set of parameters n° 1 in Table I. Regardless of the propagation vector direction (\mathbf{a} , \mathbf{b} or [110]), we find very good agreement between simulations and the data for realistic values of $\boldsymbol{\epsilon}$, m_0 and B_{ab} . Continuous lines in Figs.8 **a** and **b** show the simulations obtained when the modulation is along [110], with the external field parallel or perpendicular to the \mathbf{c} axis. The parameters are $\epsilon \simeq 0.13$, $m_0 = 0.91 \mu_B$ and $B_{ab} = 0.6 \text{ T}/\mu_B$. The obtained distribution was convoluted with a Gaussian with full width at half maximum (FWHM) 0.05 T , in order to take into account the disorder induced by the Ni substitution. Simulations are not very sensitive to the value of the incommensurate parameter if it is kept small. Good fits are obtained in the range $\epsilon \leq 0.2$.

In a similar manner, we simulated the NMR spectrum obtained for $x = 0.026$ assuming IC-SDW with the Fourier components for $x = 0.03$ in Table I and with the same $\boldsymbol{\epsilon}$ and B_{ab} values as above. Figure 8 **c** shows the simulation obtained for a modulation along [110], with $m_0 = 0.55 \mu_B$, convoluted with a Gaussian of FWHM 0.2 T . It is quite close to the experimental lineshape.

5. Discussion and Conclusion

Our ^{57}Fe Mössbauer spectroscopy measurements on the pure and Ni-doped $BaFe_2As_2$ indicate the presence of a first order transition towards a spin density wave state. In pure

‡ However, if the propagation vector $\boldsymbol{\epsilon}$ of the incommensurate modulation is parallel to the \mathbf{a} axis, the term in the Hamiltonian involving B_{ab} is zero.

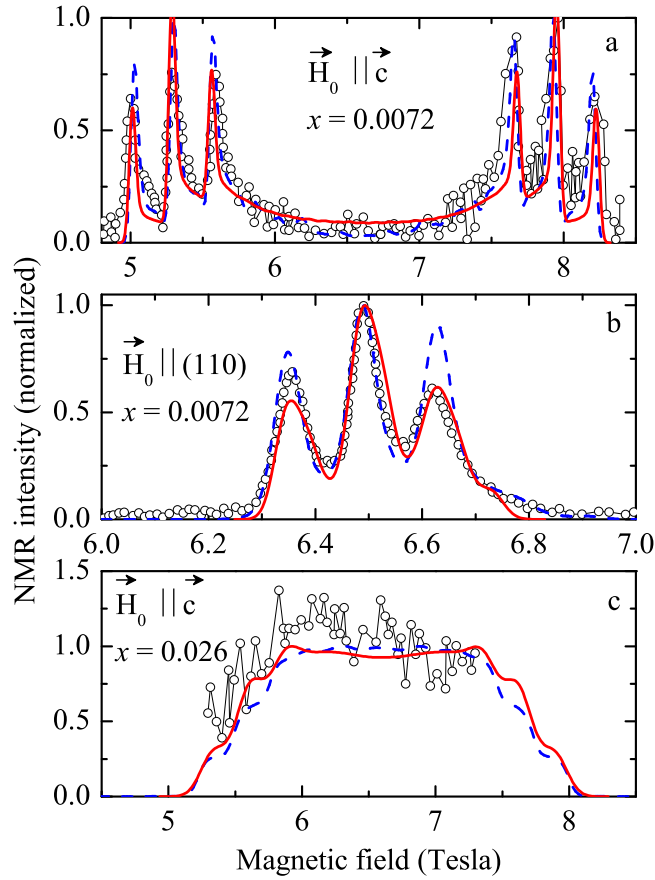


Figure 8. ^{75}As NMR spectra in $\text{Ba}(\text{Fe}_{1-x}\text{Ni}_x)_2\text{As}_2$ taken from Refs.[24, 25]. For $x=0.0072$: **a**) the external magnetic field applied parallel to the \mathbf{c} axis, and **b**) along the $[110]$ direction. For $x = 0.026$: **c**) the external magnetic field applied parallel to the \mathbf{c} axis. The solid lines are simulations with the IC-SDW model and the dashed lines are simulations with the “perturbation” model.

BaFe_2As_2 , the SDW is commensurate, in agreement with neutron scattering results, and the first order nature of the transition is in line with ^{75}As NMR results.

In $\text{Ba}(\text{Fe}_{1-x}\text{Ni}_x)_2\text{As}_2$ with $x = 0.01$ and $x = 0.03$, the magnetic phase is characterized by a broad distribution of Fe hyperfine fields. We analyzed our results in relation to NMR measurements in the framework of two different models: an incommensurate spin density wave and a dopant-induced perturbation of the Fe moments. We have shown that both ^{75}As NMR and Mössbauer spectra can be fitted well with either model, contrary to what is stated in Refs.[24, 25]. Therefore, at low doping it is not possible to conclude from the available NMR or Mössbauer data whether the “perturbation” or the IC-SDW model is relevant in Ni doped BaFe_2As_2 . At larger doping, a more elaborate model is necessary in order to track the role of disorder, because the “perturbation” model collapses even for moderate concentrations such as $x = 0.03$.

In the more studied Ba(Fe_{1-x}Co_x)₂As₂ family, the presence of IC-SDW is still a matter of debate. While IC-SDW was inferred from local techniques, resonant x-ray scattering measurements for $x = 0.047$ did not find any sign of incommensurability along \mathbf{a} or \mathbf{b} , down to relatively small values of ϵ [41]. Neutron scattering detected an IC-SDW only recently, in a small concentration range above $x = 0.056$, with a propagation vector $\boldsymbol{\epsilon}$ along \mathbf{b} and ϵ values ranging from 0.02 to 0.03 [23]. The Mössbauer spectrum for this concentration is well fitted with these parameters §. One can wonder whether IC-SDW could be present at all concentrations in the low doping regime of Ba(Fe_{1-x}Co_x)₂As₂, because the direction of the propagation vector of the modulation could change with x , following variations in the Fermi surface nesting. This would further complicate the detection of IC-SDW by neutron scattering and resonant x-ray measurements.

While disorder due to substitutions is inherent in Ba(Fe_{1-x}Ni_x)₂As₂ and Ba(Fe_{1-x}Co_x)₂As₂, there are a few stoichiometric systems in which the signature of incommensurability was observed and the presence of disorder can be ruled out. In the “122 family”, the stoichiometric system SrFe₂As₂ presents, under pressure, a crossover versus temperature from commensurate to incommensurate AF, seen by ⁷⁵As NMR measurements [18]. In NaFeAs, a similar crossover was evidenced at ambient pressure by ²³Na and ⁷⁵As NMR [42, 43]. This system presents filamentary superconductivity below 23 K and, similar to other Fe-based pnictides, shows a structural phase transition from tetragonal to orthorhombic at 50 K, followed by a magnetic one towards an antiferromagnetically ordered state at 40 K. These observations suggests that incommensurability is not only related to doping but rather, might be connected to subtle changes of the Fermi surface.

In conclusion, we have shown that at very low doping levels, both IC-SDW and dopant-induced perturbation models fit the NMR and Mössbauer spectra well in Ba(Fe_{1-x}Ni_x)₂As₂. However, the latter model collapses even for moderate dopant concentrations $x = 0.03$, because it overestimates the disorder effect. Further theoretical calculations are required in order to sort out the precise influence of the dopant on the magnetic properties of pnictides. On the other hand, the IC-SDW model successfully reproduces the spectra over the whole doping region. This, together with the observation of IC-SDW in the stoichiometric systems mentioned above and the similarity with the Co family, suggests that IC-SDW might also be present in the Ni family.

Acknowledgments

Authors wish to thank Julien Bobroff and Henri Alloul for helpful discussions and reading of the manuscript, and Sylvie Poissonnet (SRMP/CEA) for the chemical analysis of the samples. This work was supported by the ANR grant PNICTIDES. A.O. acknowledges financial support from “Triangle de la Physique”.

[1] Kamihara Y, Watanabe T, Hirano M and Hosono H 2008 *J. Am. Chem. Soc.*

§ unpublished data

- [2] Mazin I I and Schmalian J 2009 *Physica C* **469** 614
- [3] Laplace Y, Bobroff J, Rullier-Albenque F, Colson D and Forget A 2009 *Phys. Rev. B* **80** 140501
- [4] Julien M H, Mayaffre H, Horvatić M, Berthier C, Zhang X D, Wu W, Chen G F, Wang N L and Luo J L 2009 *Europhys. Lett.* **87** 37001
- [5] Luetkens H, Klauss H H, Kraken M, Litterst F J, Dellmann T, Klingeler R, Hess C, Khasanov R, Amato A, Baines C, Kosmala M, Schumann O J, Braden M, Hamann-Borrero J, Leps N, Kondrat A, Behr G, Werner J and Buchner B 2009 *Nat. Mater.* **8** 305
- [6] Lumsden M D and Christianson A D 2010 *J. Phys.: Condens. Matter* **22** 203203
- [7] Singh D, Du M H, Zhang L, Subedi A and An J 2009 *Physica C* **469** 886
- [8] Dong J, Zhang H J, Xu G, Li Z, Li G, Hu W Z, Wu D, Chen G F, Dai X, Luo J L, Fang Z and Wang N L 2008 *Europhys. Lett.* **83** 27006
- [9] Fink J, Thirupathaiah S, Ovsyannikov R, Dürr H A, Follath R, Huang Y, de Jong S, Golden M S, Zhang Y Z, Jeschke H O, Valentí R, Felser C, Dastjani Farahani S, Rotter M and Johrendt D 2009 *Phys. Rev. B* **79** 155118
- [10] Brouet V, Marsi M, Mansart B, Nicolaou A, Taleb-Ibrahimi A, Le Fèvre P, Bertran F, Rullier-Albenque F, Forget A and Colson D 2009 *Phys. Rev. B* **80** 165115
- [11] Ding H, Richard P, Nakayama K, Sugawara K, Arakane T, Sekiba Y, Takayama A, Souma S, Sato T, Takahashi T, Wang Z, Dai X, Fang Z, Chen G F, Luo J L and Wang N L 2008 *Europhys. Lett.* **83** 47001
- [12] Liu C, Samolyuk G D, Lee Y, Ni N, Kondo T, Santander-Syro A F, Bud'ko S L, McChesney J L, Rotenberg E, Valla T, Fedorov A V, Canfield P C, Harmon B N and Kaminski A 2008 *Phys. Rev. Lett.* **101** 177005
- [13] Park J T, Inosov D S, Yaresko A, Graser S, Sun D L, Bourges P, Sidis Y, Li Y, Kim J H, Haug D, Ivanov A, Hradil K, Schneidewind A, Link P, Faulhaber E, Glavatsky I, Lin C T, Keimer B and Hinkov V 2010 *Phys. Rev. B* **82** 134503
- [14] Rice T M 1970 *Phys. Rev. B* **2** 3619
- [15] Vorontsov A B, Vavilov M G and Chubukov A V 2009 *Phys. Rev. B* **79** 060508
- [16] Vorontsov A B, Vavilov M G and Chubukov A V 2010 *Phys. Rev. B* **81** 174538
- [17] Cvetkovic V and Tesanovic Z 2009 *Phys. Rev. B* **80** 024512
- [18] Kitagawa K, Katayama N, Gotou H, Yagi T, Ohgushi K, Matsumoto T, Uwatoko Y and Takigawa M 2009 *Phys. Rev. Lett.* **103** 257002
- [19] Bonville P, Rullier-Albenque F, Colson D and Forget A 2010 *Europhys. Lett.* **89** 67008
- [20] Marsik P, Kim, K W, Dubroka A, Rössle M., Malik V K, Schulz L, Wang C N, Niedermayer C, Drew A J, Willis M, Wolf T and Bernhard C 2010 *Phys. Rev. Lett.* **105** 057001
- [21] Christianson A D, Lumsden M D, Nagler S E, MacDougall G J, McGuire M A, Sefat A S, Jin R, Sales B C and Mandrus D 2009 *Phys. Rev. Lett.* **103** 087002
- [22] Pratt D K, Tian W, Kreyssig A, Zarestky J L, Nandi S, Ni N, Bud'ko S L, Canfield P C, Goldman A I and McQueeney R J 2009 *Phys. Rev. Lett.* **103** 087001
- [23] Pratt D K, Kim M G, Kreyssig A, Lee Y B, Tucker G S, Thaler A, Tian W, Zarestky J L, Bud'ko S L, Canfield P C, Harmon B N, Goldman A I and McQueeney R J 2011 *Phys. Rev. Lett.* **106** 257001
- [24] Dioguardi A P, apRoberts Warren N, Shockley A C, Bud'ko S L, Ni N, Canfield P C and Curro N J 2010 *Phys. Rev. B* **82** 140411
- [25] Dioguardi A P, apRoberts Warren N, Shockley A C, Bud'ko S L, Ni N, Canfield P C and Curro N J 2011 *arXiv: 1102.1936*
- [26] Wang P, Stadnik Z M, Zukrowski J, Thaler A, Bud'ko S L, Canfield P C 2011 *Phys. Rev. B* **84** 024509
- [27] Kreyssig A, Kim M G, Nandi S, Pratt D K, Tian W, Zarestky J L, Ni N, Thaler A, Bud'ko S L, Canfield P C, McQueeney R J, Goldman A I 2010 *Phys. Rev. B* **81** 134512
- [28] Rullier-Albenque F, Colson D, Forget A and Alloul H 2009 *Phys. Rev. Lett.* **103** 057001
- [29] Olariu A, Rullier-Albenque F, Colson D and Forget A 2011 *Phys. Rev. B* **83** 054518

- [30] Rotter M, Tegel M, Schellenberg I, Schappacher F M, Pöttgen R, Deisenhofer J, Günther A, Schrettle F, Loidl A and Johrendt D 2009 *New J. Phys.* **11** 025014
- [31] Rotter M, Tegel M, Johrendt D, Schellenberg I, Hermes W and Pöttgen R 2008 *Phys. Rev. B* **78** 020503
- [32] Nowik I, Felner I, Ni N, Bud'ko S L and Canfield P C 2010 *J. Phys.: Condens. Matter* **22** 355701
- [33] Huang Q, Qiu Y, Bao W, Green M A, Lynn J W, Gasparovic Y C, Wu T, Wu G and Chen X H 2008 *Phys. Rev. Lett.* **101** 257003
- [34] Kitagawa K, Katayama N, Ohgushi K, Yoshida M and Takigawa M 2008 *J. Phys. Soc. Jpn.* **77** 114709
- [35] Dunlap R A, Eelman D A and MacKay G R 1998 *J. Non-Cryst. Solids* **223** 141
- [36] Verma H R, Sundqvist T, Wäppling R and Arnberg L 1985 *Physica Scripta* **32** 155
- [37] Felner I and Nowik I 2011 *J. Supercond. Novel Mag.* **24**(4) 1363
- [38] Nowik I and Felner I 2009 *Physica C* **469** 485
- [39] Kemper A F, Cao C, Hirschfeld P J and Cheng H P 2009 *Phys. Rev. B* **80** 104511
- [40] Wang M, Luo H, Zhao J, Zhang C, Wang M, Marty K, Chi S, Lynn J W, Schneidewind A, Li S and Dai P 2010 *Phys. Rev. B* **81** 174524
- [41] Kim M G, Kreyssig A, Lee Y B, Kim J W, Pratt D K, Thaler A, Bud'ko S L, Canfield P C, Harmon B N, McQueeney R J and Goldman A I 2010 *Phys. Rev. B* **82** 180412
- [42] Kitagawa K, Mezaki Y, Matsubayashi K, Uwatoko Y and Takigawa M 2011 *J. Phys. Soc. Jpn.* **80** 033705
- [43] Klanjšek M, Jeglič P, Lv B, Guloy A M, Chu C W, Arčon D 2011 *Phys. Rev. B* **84** 054528